KOPIO TN093

FastMC comparison of photon veto inefficiency parametrizations

David E. Jaffe, BNL

June 21, 2004

Abstract

I compared the rates of $\mathrm{K_L^0} \to \pi^0\pi^0$, $\mathrm{K_L^0} \to \pi^0\pi^0\pi^0$, $\mathrm{K_L^0} \to e^\pm\pi^0\pi^\mp\nu$, $\mathrm{K_L^0} \to \pi^0\pi^+\pi^-$ and $\mathrm{K_L^0} \to e^\pm\pi^\mp\nu\gamma$ backgrounds for the standard KOPIO photon veto inefficiency, a 'new' photon veto inefficiency and an 'optimistic' photon veto inefficiency. The 'new' photon veto inefficiency is based on the agreement of E787 photon veto measurements and FLUKA studies for $E_\gamma > 150$ MeV. The 'optimistic' photon veto inefficiency is approximately twice as good as the 'new' photon veto inefficiency. With the 'new' ('optimistic') photon veto, the $\mathrm{K_L^0} \to \pi^0\pi^0\pi^0$ rate decreases by roughly a factor of 1.8 (20) and the $\mathrm{K_L^0} \to \pi^0\pi^0$ rate decreases by roughly a factor of 1.8 (5).

1 Introduction

This study follows the method of the study described in TN083 [1]. I have used two additional parametrizations of the photon veto inefficiency. The two parametrizations are dubbed 'new' and 'optimistic'. The 'new' photon veto inefficiency is based on the agreement of E787 photon veto measurements and FLUKA studies for $E_\gamma > 150$ MeV shown in TN088 [2]. For $E_\gamma < 150$ MeV, the 'new' photon veto inefficiency merges smoothly with the 'standard' photon veto inefficiency. The 'optimistic' photon veto inefficiency was created based on the suggestion of Andries van der Schaaf and is a factor of two better than the 'new' photon veto inefficiency for $E_\gamma > 20$ MeV. For $E_\gamma < 20$ MeV, the 'optimistic' photon veto inefficiency approaches the 'new' and 'standard' photon veto inefficiency because all are constrained to have unit inefficiency at zero photon energy. Figures 1 and 2 show the 'standard', 'new' and 'optimistic' photon veto inefficiency as a function of photon energy as well as the FLUKA results for a threshold of 1 MeV visible energy [2].

Some additional differences between this note and TN083 [1] are that I have used version v1_2 of the FastMC [3] with the "Bryman" PR model for these results [3]. The "Zeller" PR model was used for the results in TN083 [1]. In addition the decay region is farther downstream and the aperture of the downstream beam hole is larger. A collimation system, extended target and $\mathrm{K_L^0}$ beam with angular dependence are also used. These modifications and the results for the signal and background rates are described in TN092 [4].

2 Results and conclusions

The calculated rates for signal and $K^0_L \to \pi^0\pi^0$, $K^0_L \to \pi^0\pi^0\pi^0$, $K^0_L \to e^\pm\pi^0\pi^\mp\nu$, $K^0_L \to \pi^0\pi^+\pi^-$ and $K^0_L \to e^\pm\pi^\mp\nu\gamma$ backgrounds with the "Bryman" PR model [3] are given in Table 1. The improvement in the photon veto inefficiency for $E_\gamma > 150$ MeV (the 'new' photon veto) would reduce the $K^0_L \to \pi^0\pi^0$ and $K^0_L \to \pi^0\pi^0\pi^0$ background by approximately a factor of 1.6 to 2.0 depending on the cuts. A factor of two improvement in the 'new' photon veto would give a dramatic decrease in the $K^0_L \to \pi^0\pi^0$ rate of five and in the $K^0_L \to \pi^0\pi^0\pi^0$ rate of twenty. The impact of such reductions in the photon backgrounds would be more fully assessed by re-optimization of the cuts targetted at the $K^0_L \to \pi^0\pi^0$ background.

References

[1] D.E. Jaffe, *FastMC comparison of standard and E787 photon veto inefficiency* KOPIO TN083, 14 Apr 2004.

[2] V. Burtovoy, *The generation of the photon detection inefficiency in the lead scintillator counter by the Fluka program*, KOPIO TN088, 11 May 2004.

[3] D.E. Jaffe, *FastMC User Manual*, KOPIO TN089, 27 May 2004. Also see `http://www.phy.bnl.gov/~djaffe/KOPIO/fastmc/Documentation.html` for the most up-to-date version.

[4] D.E. Jaffe, *Some FastMC acceptance and background studies*, KOPIO TN092, 9 June 2004.

Mode	Standard PV	New PV	Optimistic PV	Cut
kpnn	29.25 ± 0.4126	29.25 ± 0.4126	29.25 ± 0.4126	MZ
kpnn	98.58 ± 0.7540	98.58 ± 0.7540	98.58 ± 0.7540	AK basic
kpnn	64.77 ± 0.6115	64.77 ± 0.6115	64.77 ± 0.6115	AK loose
kpnn	56.97 ± 0.5735	56.97 ± 0.5735	56.97 ± 0.5735	AK lominal
kpnn	39.06 ± 0.4747	39.06 ± 0.4747	39.06 ± 0.4747	AK tight
kpnn	25.72 ± 0.3850	25.72 ± 0.3850	25.72 ± 0.3850	AK tighter
kpnn	22.20 ± 0.3579	22.20 ± 0.3579	22.20 ± 0.3579	AK tightest
kp3	0.7565 ± 0.06472	0.3805 ± 0.05154	0.03603 ± 0.007315	MZ
kp3	2.189 ± 0.4306	1.376 ± 0.4313	0.1618 ± 0.06502	AK basic
kp3	1.043 ± 0.1030	0.5508 ± 0.09182	0.05368 ± 0.01199	AK loose
kp3	1.042 ± 0.1030	0.5506 ± 0.09182	0.05367 ± 0.01199	AK lominal
kp3	0.7689 ± 0.09504	0.4121 ± 0.08357	0.04143 ± 0.01103	AK tight
kp3	0.5557 ± 0.09027	0.3119 ± 0.08162	0.03197 ± 0.01082	AK tighter
kp3	0.5260 ± 0.09012	0.2994 ± 0.08156	0.03107 ± 0.01082	AK tightest
kp2	3.587 ± 0.2565	2.061 ± 0.1824	0.5943 ± 0.06345	MZ
kp2	109.8 ± 5.062	65.29 ± 4.063	23.20 ± 2.010	AK basic
kp2	43.14 ± 2.775	23.48 ± 1.716	7.611 ± 0.8401	AK loose
kp2	27.08 ± 2.435	14.28 ± 1.122	4.563 ± 0.5418	AK lominal
kp2	10.67 ± 1.718	6.016 ± 0.9292	2.098 ± 0.4567	AK tight
kp2	2.199 ± 0.1910	1.288 ± 0.1391	0.3812 ± 0.05232	AK tighter
kp2	1.542 ± 0.1406	0.9005 ± 0.1043	0.2656 ± 0.03975	AK tightest
ke4	1.749 ± 1.232	1.749 ± 1.232	1.749 ± 1.232	MZ
ke4	4.228 ± 1.843	4.228 ± 1.843	4.228 ± 1.843	AK basic
ke4	2.596 ± 1.464	2.596 ± 1.464	2.596 ± 1.464	AK loose
ke4	2.593 ± 1.464	2.593 ± 1.464	2.593 ± 1.464	AK lominal
ke4	2.583 ± 1.464	2.583 ± 1.464	2.583 ± 1.464	AK tight
ke4	1.747 ± 1.232	1.747 ± 1.232	1.747 ± 1.232	AK tighter
ke4	1.745 ± 1.232	1.745 ± 1.232	1.745 ± 1.232	AK tightest
ke3g	3.679 ± 0.3595	3.679 ± 0.3595	3.560 ± 0.3518	MZ
ke3g	16.47 ± 0.8194	16.47 ± 0.8194	15.96 ± 0.8022	AK basic
ke3g	8.399 ± 0.5933	8.399 ± 0.5933	8.127 ± 0.5801	AK loose
ke3g	7.400 ± 0.5546	7.400 ± 0.5546	7.153 ± 0.5421	AK lominal
ke3g	4.818 ± 0.4343	4.818 ± 0.4343	4.644 ± 0.4236	AK tight
ke3g	2.733 ± 0.2852	2.733 ± 0.2852	2.635 ± 0.2778	AK tighter
ke3g	2.459 ± 0.2738	2.459 ± 0.2738	2.372 ± 0.2670	AK tightest
kcp3	0.5321 ± 0.1339	0.5321 ± 0.1339	0.5321 ± 0.1339	MZ
kcp3	17.02 ± 0.7295	17.02 ± 0.7295	17.02 ± 0.7295	AK basic
kcp3	1.852 ± 0.2402	1.852 ± 0.2402	1.852 ± 0.2402	AK loose
kcp3	1.852 ± 0.2402	1.852 ± 0.2402	1.852 ± 0.2402	AK lominal
kcp3	1.205 ± 0.1979	1.205 ± 0.1979	1.205 ± 0.1979	AK tight
kcp3	0.4814 ± 0.1267	0.4814 ± 0.1267	0.4814 ± 0.1267	AK tighter
kcp3	0.3268 ± 0.09615	0.3268 ± 0.09615	0.3268 ± 0.09615	AK tightest

Table 1: The calculated rates and statistical uncertainties for the signal (kpnn), $K^0_L \rightarrow \pi^0\pi^0\pi^0$ (kp3), $K^0_L \rightarrow \pi^0\pi^0$ (kp2), $K^0_L \rightarrow e^\pm\pi^0\pi^\mp\nu$ (ke4), $K^0_L \rightarrow e^\pm\pi^\mp\nu\gamma$ (ke3g) and $K^0_L \rightarrow \pi^0\pi^+\pi^-$ (kcp3) backgrounds for various sets of cuts for the standard, new and optimistic photon veto inefficiency.

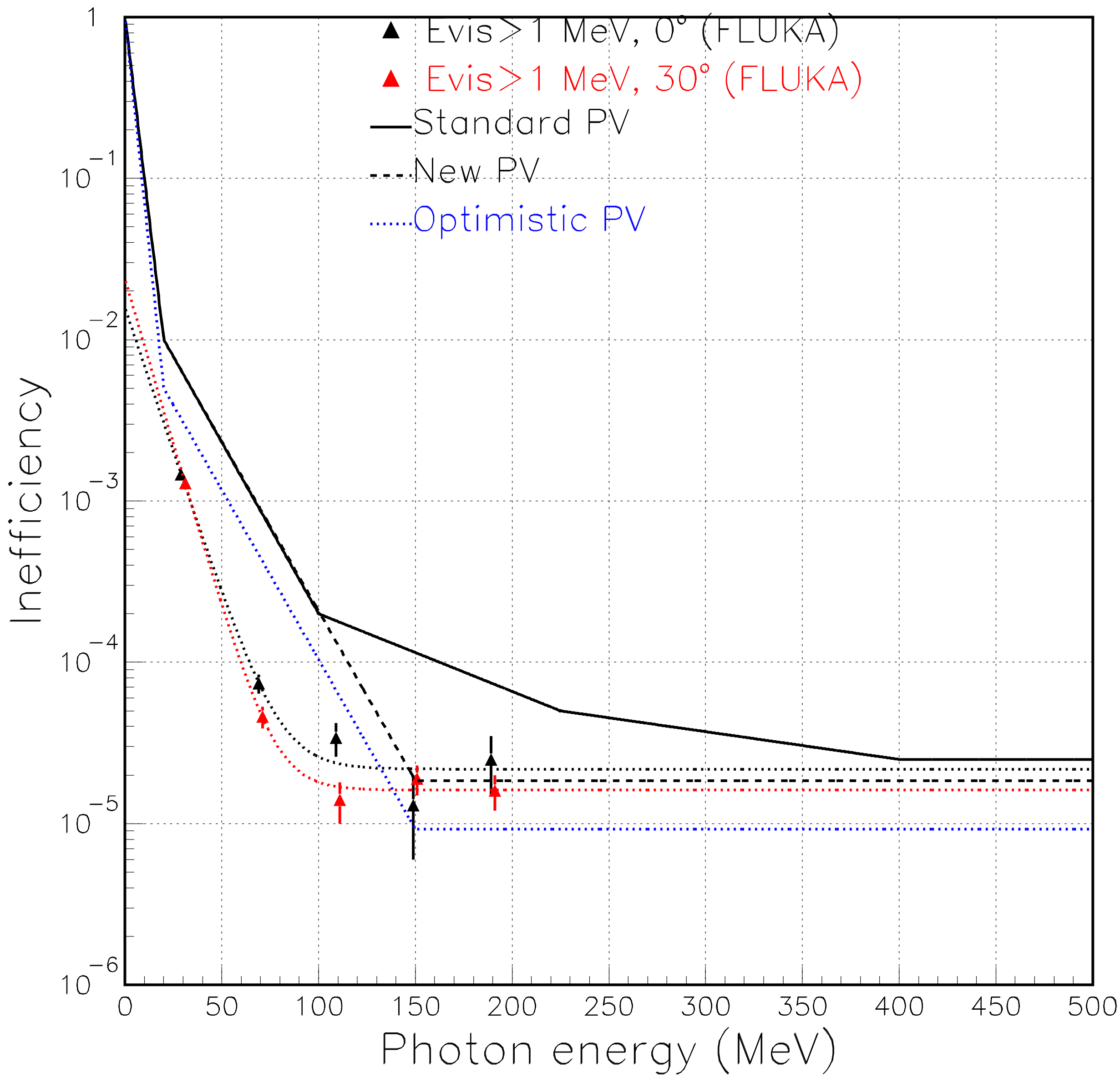

Figure 1: The 'standard' (solid), 'new' (dashed) and optimistic (blue dotted) photon veto inefficiency as a function of photon energy. The points are taken from TN088 [2] for 0° and 30° incident photon angles for a 1 MeV visible energy threshold with the FLUKA simulation. The black and red dotted curves are fits to the FLUKA results with the sum of an exponential and a zeroth-order polynomial for 0° and 30° incident photon angles, respectively.

2004/06/18 12.30

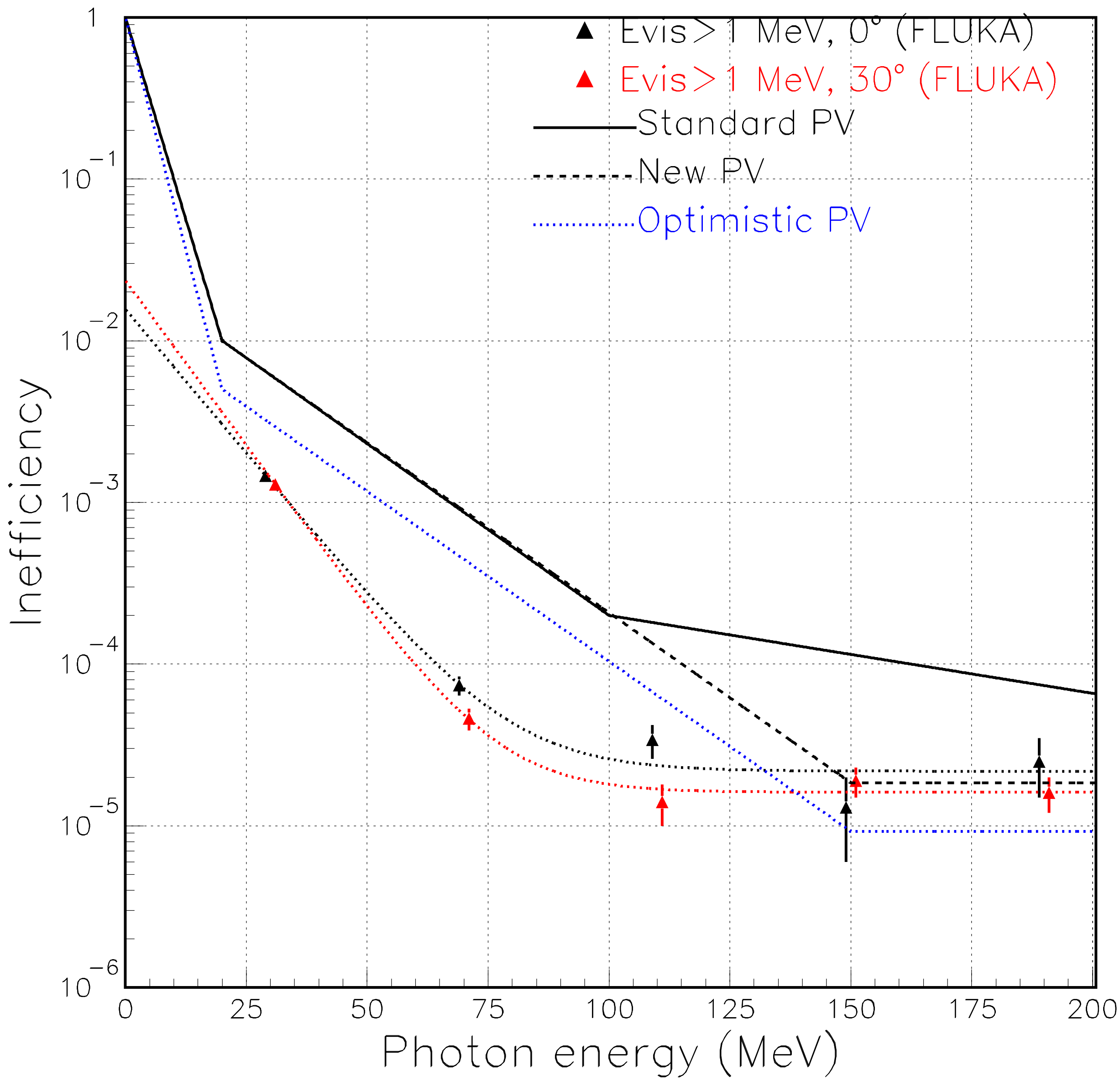

Figure 2: Same as Figure 1 but emphasizing the low energy region.